Clays and Clay Minerals, Vol. 38, No. 6, 600–608, 1990.

PARAMAGNETIC DEFECT CENTERS IN HYDROTHERMAL KAOLINITE FROM AN ALTERED TUFF IN THE NOPAL URANIUM DEPOSIT, CHIHUAHUA, MEXICO

JEAN-PIERRE MULLER,[1,3] PHILIPPE ILDEFONSE,[2,3] AND GEORGES CALAS[3]

[1] O.R.S.T.O.M., Département T.O.A., 75480 Paris Cedex 10, France

[2] U.F.R. Sciences Physiques de la Terre, Université Paris 7
2 Place Jussieu, 75251 Paris Cedex 05, France

[3] Laboratoire de Minéralogie-Cristallographie, UA CNRS 09, Universités Paris 6 et 7
4 Place Jussieu, 75252 Paris Cedex 05, France

Abstract—Point defect centers in hydrothermal kaolinite have been investigated using electron paramagnetic resonance (EPR). Kaolinite was sampled in petrographically well-defined materials coming from uranium-rich hydrothermally altered volcanic tuffs (Nopal I uranium deposit, Chihuahua, Mexico), which show extensive kaolinization and an intense redistribution of uranium. Several kaolinite parageneses were defined according to their origin (fissure fillings and feldspar pseudomorphs); their location relative to the U^{6+} mineralization at the scale of the deposit (mineralized breccia pipe vs. barren surrounding rhyolitic tuffs), and at the scale of mineral assemblages; and their crystal chemistry.

Two types of centers of axial symmetry were identified (A- and A′-centers) and represent positive holes trapped on apical oxygens (Si–O^--centers). A-centers were stable to 400°C, whereas A′-centers annealed at 350°C. A relation between defect-center concentration and U content demonstrates that natural irradiation was responsible for these centers. On the other hand, defect-center concentration was not directly linked to the origin (fissural or feldspar pseudomorph) or the crystal chemistry (structural order and substitutional Fe^{3+} content) of the kaolinite. According to petrographic data, and with respect to the relative thermal stability of A- and A′-centers, two successive irradiations of kaolinite were evidenced: (1) originally during crystallization of kaolinite from radioactive hydrothermal solutions, and (2) permanently when kaolinite was in contact with secondary U-silicates, which led to the formation of A′-centers.

Because of the short half-life of U, these two radiation-induced centers were created by short-lived elements of the U-decay series. As a consequence, variations of defect-center concentration possibly reflect variations in radioactive disequilibrium during the history of the alteration system. This provides a unique tool for tracing the dynamics of the transfer of radionuclides in the geosphere: kaolinite may be used as a sensitive *in situ* dosimeter, which may be useful in the fields of weathering petrology and nuclear waste management.

Key Words—Defect centers, Electron paramagnetic resonance, Hydrothermal, Kaolinite, Natural radiation.

INTRODUCTION

Kaolinites are known to incorporate defects of various types, either extended (e.g., stacking faults) or localized (e.g., impurities), which are related to their formation conditions (cf. reviews by Hall, 1980; Cases *et al.*, 1982; Giese, 1988). Paramagnetic defect centers have been known in kaolinite since the pioneering study of Meads and Malden (1975). Paramagnetic defect centers, however, have been only recently correlated with geochemical and petrological parameters: successive generations of kaolinites have been sampled from the same lateritic profile and the concentration of defect centers have been found to be strongly sample dependent, in relation to the Fe and U-Th contents of bulk samples (Muller and Calas, 1989). By taking into account the efficient chemisorption of uranium and its decay elements on iron oxide precursors (i.e., ferric gels), these defects have been attributed to an irradiation of the kaolinite associated with iron-accumulation processes during the first stages of weathering. The evolution of iron oxides towards a greater crystallinity causes radioactive elements to be desorbed and leached during further stages of soil differentiation. Stable defect centers remain as a memory of the transit of radionuclides.

The purpose of this paper is (1) to confirm that natural irradiation is at the origin of point defect centers in kaolinite and (2) to test the potential use of these defects to detect radionuclide migration in the geosphere. With these objectives in view, investigations have been carried out on petrographically well-defined materials from uranium-rich hydrothermally altered volcanic tuffs, which show extensive kaolinization as well as intense redistribution of uranium.

MATERIALS AND METHODS

Materials

The studied uranium mineral deposit (Nopal I) is located in the Sierra Peña Blanca, Chihuahua, Mexico (Goodell, 1981), in which > 100 radiometric anomalies

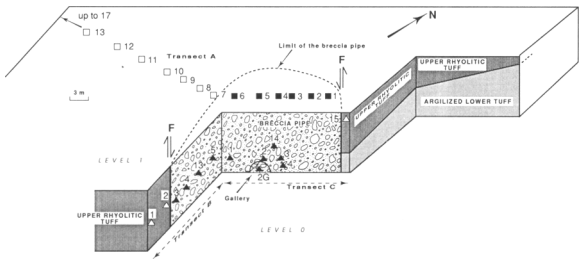

Figure 1. Schematic representation of the quarry (level 0 of Figure 2) and location of samples along the transects A, B, and C.

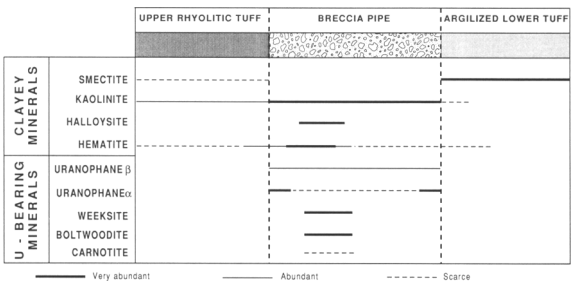

Figure 2. Nature, location, and relative abundance of the main secondary parageneses of clay and U-bearing minerals.

have been identified in Tertiary volcanic rocks. The Sierra Peña Blanca is a volcanic range 60 km long and 30 km wide in northern Mexico. This range consists of gently dipping Tertiary volcanic rocks, which overlie a calcareous basement of Cretaceous age (Alba and Chavez, 1974; Magonthier, 1984; Cardenas-Flores, 1985). Uranium mineralized bodies have been recognized near the bottom of the volcanic suite (44 million years old). Three genetic types of ore have been identified: hydrothermal, supergene, and mixed (George-Aniel *et al.*, 1985). The Nopal I vein-type deposit belongs to the first type and was chosen for this study because of its intense kaolinization during hydrothermal alteration (Calas, 1977; Leroy *et al.*, 1987).

The Nopal formation consists of an upper, welded rhyolitic tuff and a lower, weakly welded tuff, which are cut by an irregular breccia pipe (100 m vertical extent; 20–40 m wide) (Cortes *et al.*, 1980; Aniel, 1983; Figure 1). East of the pipe, a normal fault brings the two types of tuffs into contact (Figure 1). The rhyolitic tuff is mainly kaolinized: the kaolinization, prevalent in the breccia zone, decreases with distance from this zone and with a decrease in the density of fractures (Figure 2). In contrast, lower tuff alteration consists mainly of dioctahedral smectite coexisting with some zeolites (Figure 2). The uraniferous mineralization, estimated to be 5–6 million years old (Chaulot-Talmon, 1984), is strictly located in the breccia zone and appears as an assemblage of U^{6+} minerals (α- and β-uranophane, weeksite, boltwoodite; Figure 2) and yellow to green opal (Aniel, 1983; George-Aniel *et al.*, 1985; Ildefonse *et al.*, 1988).

Sampling

Preliminary analysis of the distribution and abundance of the principal secondary minerals linked to hydrothermal alteration (kaolinite, smectite, U-bearing minerals; Ildefonse *et al.*, 1988) was carried out on levels 0 and 1 of the quarry (Figure 1). The altered rhyolitic tuff was carefully sampled so as to preserve the petrographic structures. Samples were collected along three transects (Figure 1): transect A, 75 m long, on level 1; transect B, 15 m long and paralleling the rim of the pipe, and transect C, 18 m long and cross-cutting the pipe, on level 0.

Methods

Undisturbed subsamples were impregnated with epoxy resin and thin-sectioned for petrographic observations. Based on thin sections and fracture-surface observations, samples were selected for the study of specific features using scanning electron microscopes (SEMs) operating at 20 kV (JSM 20 and S 200 C coupled with a LINK energy-dispersive X-ray spectrometer). Specimens were mounted on brass stubs and coated with gold. Undisturbed samples were broken to expose fresh surface for coating. Kaolinite was hand-picked under a stereomicroscope.

X-ray powder diffraction (XRD) data were obtained using a PW 1710 vertical goniometer and monochromatic CuKα radiation (40 kV, 30 mA) at scanning rates of 1°2θ/min or a Guinier camera for uranium-bearing mineral determination. The crystallinity of the kaolinite samples was estimated by infrared spectroscopy (IR) using a Fourier-Transform IR Nicolet 5DX spectrometer (Muller and Bocquier, 1987). Peak intensities were calculated after baseline correction. A quantitative relation exists between the relative intensity of the bands at 3669 and 3649 cm^{-1} and the crystal order of kaolinite, as measured, for example, by the Hinckley index (Cases *et al.*, 1982). This relation has led to the definition of a "disorder index" [DI(IR)] as the ratio of the apparent intensities of two bands [I(3669)/I(3649)] which, according to previous observations on soil kaolinites (Muller and Bocquier, 1987), increased with decreasing degree of order.

Electron paramagnetic resonance (EPR) spectroscopy (Calas, 1988, and references therein) was used to study the two types of paramagnetic centers in the structure of kaolinite: point defect centers (Muller and Calas, 1989, and references therein) and Fe^{3+} replacing Al^{3+} in two sites of the octahedral sheet (Muller and Bocquier, 1987, and references therein). The measurements were made at X-band (9.27 GHz) and room temperature on a CSE 109 Varian spectrometer, using a 100-kHz modulation. A 40-mW microwave power

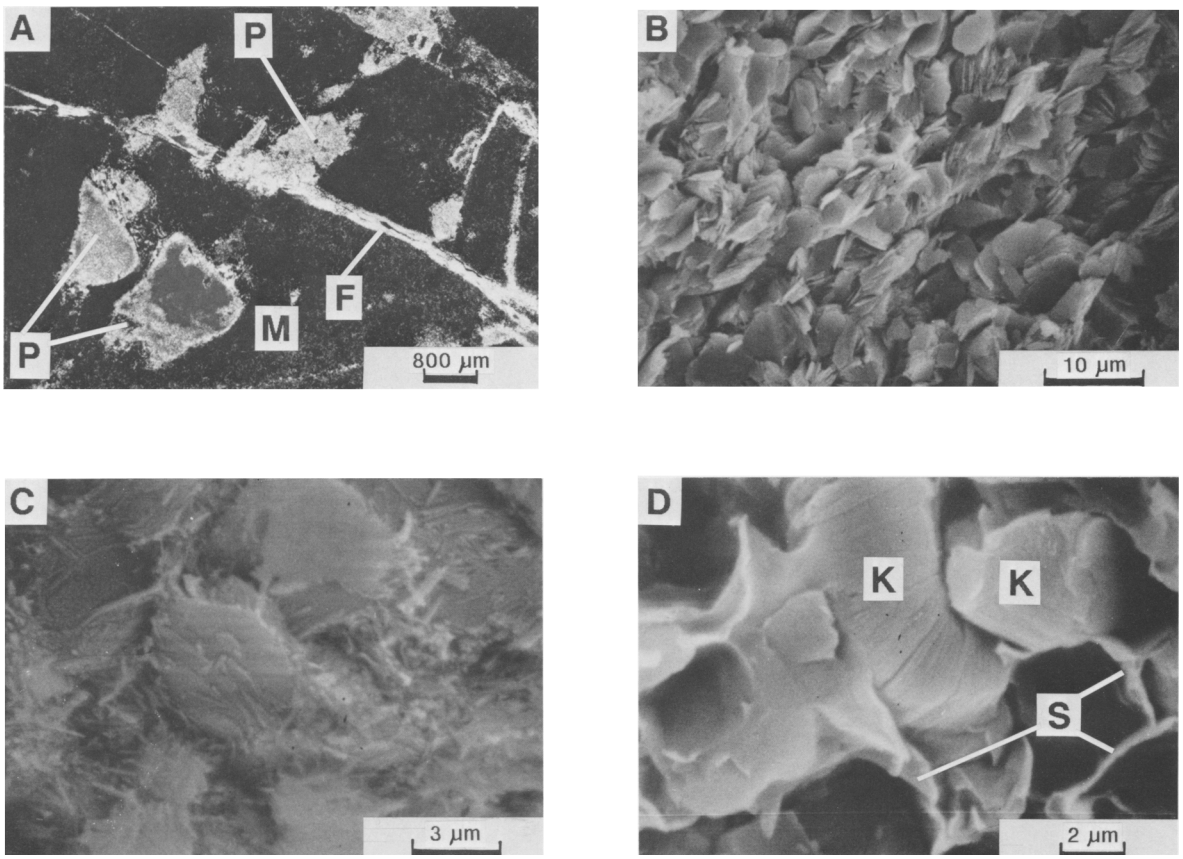

Figure 3. (A) Photomicrograph of clay minerals in feldspar phenocrysts pseudomorphs (P) and in fissures (F) in breccia pipe ground mass (M). (B) Scanning electron micrograph (SEM) of tightly packed euhedral hexagonal flakes of kaolinite. (C) SEM of halloysite elongate particles covering kaolinite flakes. (D) SEM of kaolinite flakes (K) intimately coexisting with thin, undulated smectitic tactoides (S).

was chosen because of the absence of EPR signal saturation. g-values were calibrated by comparison with a standard (DPPH, g = 2.0036), and quantitative determination was possible by using the same amount of sample (50 mg) filling calibrated silica tubes. Most samples were pretreated by the complexing procedure of De Endredy (1963) to remove iron oxides (Muller and Calas, 1989). Because the samples investigated here had the same kind of centers, EPR spectra presented a similar shape. Subsequently, the concentration of the paramagnetic centers was estimated using a simplified procedure (Calas, 1988): because the experimental parameters were held constant, the concentration of paramagnetic centers was assumed to be proportional to $S = \Delta B^2 I$, where ΔB is the linewidth peak-to-peak and I the signal intensity (cf. Figure 8b). Three S parameters, expressed in arbitrary units, were calculated: S(i) and S(e) estimated the concentration of substitutional Fe^{3+} in two sites (Meads and Malden, 1975) giving rise to "internal" and "external" EPR signals, respectively (Mestdagh *et al.*, 1980); S(d) parameter, estimated the concentration of point defect centers. The U and Th contents of the kaolinite samples were determined by inductively coupled plasma-emission spectrometry (Govindaraju, 1973).

RESULTS AND DISCUSSION

Clay minerals parageneses

Clay minerals occurred (1) in pseudomorphs of feldspar phenocrysts (Figure 3A), in the mineralized breccia pipe and in the surrounding barren rhyolitic tuff, and (2) in fissures (Figure 3A) in the breccia pipe. Kaolinite was the major clay mineral encountered. It existed as tightly packed, euhedral hexagonal flakes (5 μm in diameter) (Figure 3B), a habit considered to be typically hydrothermal (Keller, 1976). In the center of the pipe, kaolinite flakes were covered with elongated particles of halloysite (Figure 3C) in fissure fillings and in feldspar pseudomorphs. Outside the breccia pipe, kaolinite flakes intimately coexisted with thin, undulate smectitic tactoids (Figure 3D). Most clay samples were free of iron oxides, except for some feldspar pseudomorphs on the northwest side of the pipe (samples

https://doi.org/10.1346/CCMN.1990.0380605 Published online by Cambridge University Press

Table 1. Location and characteristics of the samples studied.

Sample	u	h	s	Distance (m)	DI(IR)	S(i)	S(e)	S(d)	U (ppm)	Th (ppm)
Fissures										
C15				0.00	0.93	3	90	133	58.8	2.8
C4*		x		10.40	0.93	16	208	433	1262.0	0.1
C3*	x			10.55	0.91	16	167	483	2007.8	2.6
C14*	x	x		11.50	0.87	17	230	416	4396.9	0.1
C2*	x	x		13.40	0.93	15	252	285	3240.5	0.1
C2G*	x			13.55	0.94	4	140	245	1515.3	0.5
C1*				18.00	0.94	4	194	475	150.4	3.4
B5*				18.20	0.93	2	181	340	98.2	3.6
B13*	x			18.40	0.93	5	114	537	2228.2	13.5
B4*	x			19.00	0.93	3	86	339	2897.4	0.1
B3*				19.50	0.93	1	68	305	128.7	3.6
B2				20.00	0.96	2	108	169	49.0	14.9
B1				24.00	0.92	4	148	98	23.6	5.2
Pseudomorphs of feldspar										
A1*	x			2.30	0.96	3	39	568	1797.0	5.7
A2*				5.00	0.94	4	77	506	61.5	11.8
A3*				8.40	0.97	7	111	280	932.0	5.5
A4a*				10.70	0.92	8	301	471	51.5	1.6
A4b*		x		10.70	0.87	43	630	86	150.7	6.3
A5*				13.70	0.94	8	273	218	88.8	4.1
A6a*				17.70	0.95	4	118	306	123.0	6.0
A6b*				17.70	0.95	10	312	309	650.0	4.7
A7			x	21.20	0.92	3	53	128	24.3	9.1
A8			x	23.60	1.00	3	54	62	15.9	5.1
A9			x	26.40	0.97	4	612	159	21.2	31.9
A10			x	29.30	0.99	4	79	68	14.3	3.2
A11			x	33.20	0.98	4	98	166	8.4	8.9
A12			x	37.50	0.99	10	114	32	9.5	10.9
A13			x	42.60	0.99	9	133	17	6.8	9.2
A14			x	48.60	1.05	12	156	16	9.6	10.3
A15			x	55.50	1.10	10	217	23	22.9	11.1
A16			x	62.80	1.05	9	215	17	16.4	14.1
A17			x	71.00	1.01	18	469	20	10.9	16.8

* = Samples within the breccia pipe; u = identified by X-ray powder diffraction; h = halloysite; s = smectite; Distance (m) = distance in meters from the northeast limit of the breccia pipe; DI(IR) = infrared disorder index; S(i) and S(e) = substitutional Fe^{3+} content in the two sites of kaolinite lattice (a.u.) (after Mestdagh *et al.*, 1980); S(d) = defect center concentration (a.u.); U (ppm) = uranium content in bulk samples (expressed in ppm); Th (ppm) = thorium content in bulk samples (expressed in ppm).

A4b and A6b in Table 1 and Figure 1), which were impregnated with hematite ($\leq 5\%$ Fe_2O_3).

U-bearing minerals parageneses

Primary U^{4+} mineralization was recognized by Calas (1977) and George-Aniel *et al.* (1985). They reported several remobilization stages, which resulted in a complex assemblage of secondary U-bearing minerals (Figure 2). U^{6+}-bearing minerals (uranyl silicates) occurred as fissure fillings cross-cutting the kaolinite (Figure 4A) or millimeter-size patches in the breccia pipe (Ildefonse *et al.*, 1989). K-bearing minerals (weeksite, boltwoodite, and minor carnotite) dominated in the center of the pipe, whereas Ca-bearing α-uranophane was concentrated in the rims (Figure 2; Ildefonse *et al.*, 1988). Weeksite and boltwoodite were found either in fissures or in the ground mass, whereas α-uranophane was identified only in fissure fillings. α-uranophane, weeksite, and carnotite were often encountered intimately mixed with kaolinite flakes in fissure fillings (Figure 4B). The last U^{6+}-mineralization, which overlaid or crossed kaolinite fillings in fissures, consisted of β-uranophane, locally covered by a final deposit of opal (Ildefonse *et al.*, 1988). Special care was devoted to the relationships between these minerals in the hydrothermally altered upper rhyolitic tuff because the uranium remobilization is extremely important to the radiation history of associated kaolinite materials.

Defect centers in kaolinites

All EPR spectra showed an asymmetric doublet [$g_{\parallel} = 2.049$ ($\Delta g_{\parallel} = \pm 0.002$) and $g_{\perp} = 2.007$ ($\Delta g_{\perp} = \pm 0.001$); Figure 5a], devoid of resolved hyperfine structure at liquid nitrogen temperature. This doublet characterizes unambiguously the ubiquitous A-centers in natural kaolinite (Muller and Calas, 1989, and references therein). A-centers have been interpreted as $Si–O^-$-centers, i.e., positive holes trapped on an apical oxygen and oriented

https://doi.org/10.1346/CCMN.1990.0380605 Published online by Cambridge University Press

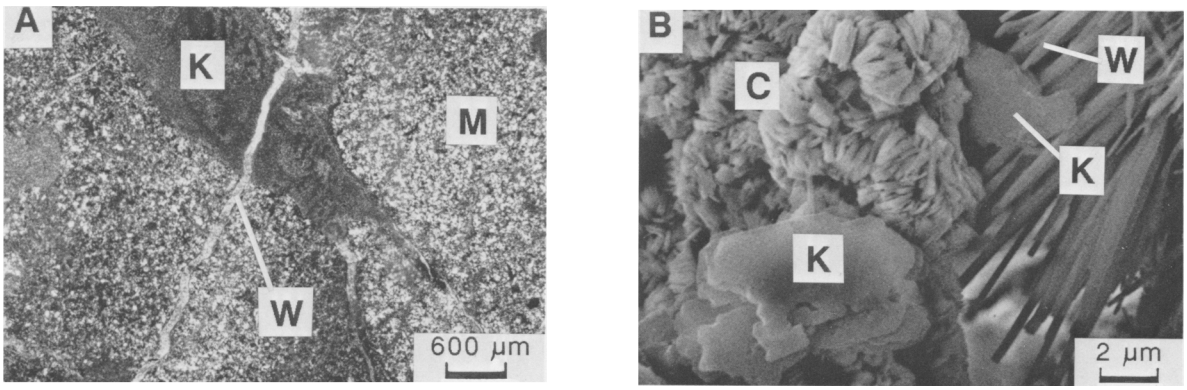

Figure 4. (A) Photomicrograph of weeksite fissure fillings (W) cross-cutting kaolinite fissure filling (K); M = ground mass. (B) Scanning electron micrograph of acicular crystals of weeksite (W) and crystals of carnotite (C) intimately mixed with kaolinite flakes (K).

perpendicular to the *ab* plane. Similar paramagnetic defect centers have been described in a large number of minerals (Marfunin, 1979). A centers are stabilized by a local positive-charge deficiency, e.g., divalent metal ion (most likely Mg^{2+} or Fe^{2+}) substituting for octahedral Al or octahedral vacancies (Angel *et al.*, 1974; Meads and Malden, 1975). Kaolinite coexisting with U-bearing minerals (see Table 1) showed an additional strong resonance (g = 2.039; Figure 5b) referred to as an A′-center.

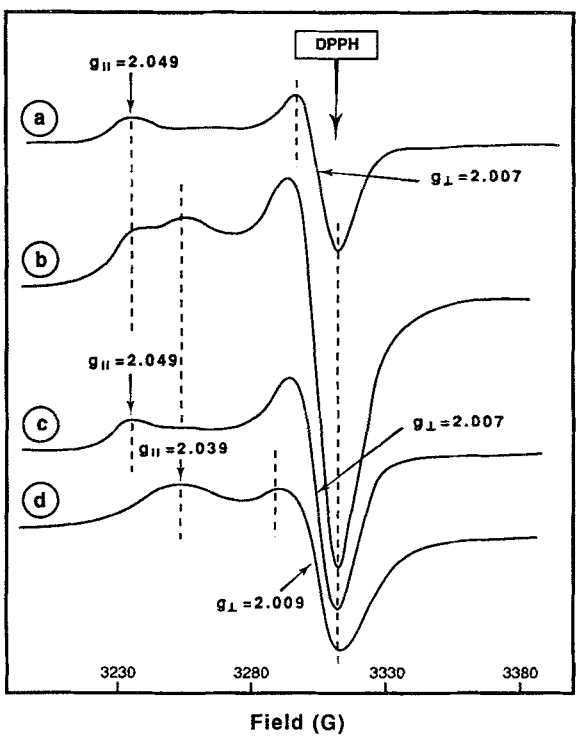

Figure 5. Comparative electron paramagnetic resonance spectra in the g = 2 region of (a) kaolinite from fissure outside of breccia pipe (sample B1), (b) kaolinite from fissure inside breccia pipe (sample C3), (c) kaolinite from sample C3 after annealing at 350°C (spectrum corresponding to A-center), (d) spectrum of A′-center obtained after subtraction of spectrum "c" from spectrum "b."

The influence of coexisting minerals on the observed EPR spectra was examined. U-bearing minerals were handpicked under binocular lens and smectites were extracted by a granulometric procedure. U-bearing minerals gave distinguishable EPR signals (not shown), which partly overlapped the doublet characteristic of kaolinite, although this phase was not detected with XRD. Some of these signals were as intense as those of kaolinite from the breccia pipe (see below); however, the contribution of U-bearing minerals to the EPR spectra of the kaolinite samples may be neglected by considering the concentration of U in the samples studied (<4400 ppm, Table 1). Smectites presented only a weak and narrow resonance.

A-centers were stable to 400°C, but A′-centers annealed at 350°C (Figure 5c). The EPR spectrum of an A′-center was obtained by the difference between the EPR spectra before and after annealing. The resulting asymmetric doublet (Figure 5d) characterized a center of axial symmetry that had EPR parameters distinct from those of the A center [$g_{\parallel}$ = 2.039 ($\Delta g = \pm 0.002$) and $g_{\perp}$ = 2.009 ($\Delta g = \pm 0.001$)]. Because the corresponding resonances were devoid of apparent hyperfine structure at liquid nitrogen temperature, this center is probably a second type of Si–O^--center.

Concentration of defect centers as a function of kaolinite location

The S(d) parameter estimates the defect center concentration, including contributions of both A- and A′-centers. Two sets of samples appear to be clearly separated on the plots (Figure 6) representing the variation of S(d) as a function of location and origin of kaolinite: (1) kaolinite samples from the breccia pipe that exhibit

https://doi.org/10.1346/CCMN.1990.0380605 Published online by Cambridge University Press

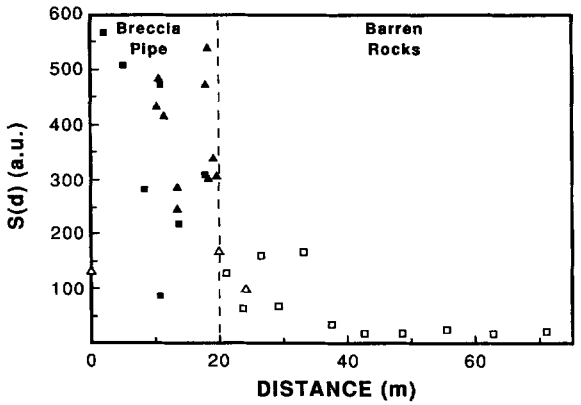

Figure 6. Variations of defect-centers concentration [estimated by S(d) parameter] vs. distance from the northeast limit of breccia pipe. ▲ = fissural kaolinite inside breccia pipe; △ = fissural kaolinite outside breccia pipe; ■ = feldspar pseudomorphs inside breccia pipe; □ = feldspar pseudomorphs outside breccia pipe.

high values of S(d) (200–600 arbitrary units), and (2) kaolinite samples from the surrounding upper barren rhyolitic tuff that are characterized by smaller S(d) values (15–100 a.u. for most samples), which progressively decrease with distance from the breccia pipe. The origin of kaolinite (fissural or feldspar pseudomorph) is not a controlling parameter with respect to the major influence of the distance from the mineralized pipe. Moreover, the defect-center concentrations encountered in these altered tuffs are significantly larger than those determined for kaolinites from weathering environments (Muller and Calas, 1989).

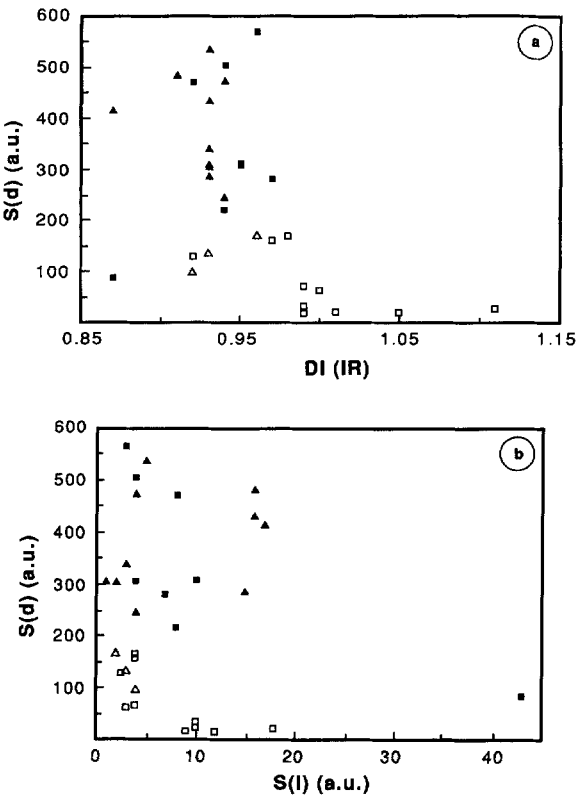

Figure 7. Plot of defect-center concentration [S(d)] for kaolinite from different location vs. (A) infrared disorder index [DI(IR)], and (B) Fe^{3+} concentration in "internal" site [estimated by S(i) parameter]. For identification of symbols, see Figure 6.

Defect-center concentration and kaolinite crystal chemistry

IR disorder indexes [DI(IR)] for kaolinite are presented in Table 1. Most DI(IR) values are <1.0, i.e., significantly less than those reported for soil kaolinites (typically 1.0 to 1.3; Muller 1988). As expected, these values suggest well-ordered kaolinite; however, a slight increase of disorder was observed from the core of the breccia pipe to the surrounding rocks, where values >1 correspond to kaolinite pseudomorphs after feldspars intimately mixed with smectite (Table 1). The plot of the variation of S(d) values of kaolinite samples from different locations as a function of DI(IR) (Figure 7a) shows that S(d) varied considerably for a given value of DI(IR). Thus, defect-center concentration and disorder degree are not directly linked.

Substitutional Fe in the kaolinite samples studied was apparently low because: (1) the EPR signals in the $g = 4$ region, which correspond to substituted trivalent iron (Meads and Malden, 1975), were weak (Figure 8a); and (2) no Fe^{2+} was detected by Mössbauer spectroscopy (A. Decarreau, University of Poitiers, Poitiers France; personal communication). S(i) and S(e) values for kaolinites are presented in Table 1. For most samples, S(i) and S(e) were in the range 2–15 and 40–300 arbitrary units, respectively. The exceptions were samples in which kaolinite coexisted with halloysite in the breccia pipe or with smectite in the barren rhyolitic tuff. In comparison, values of S(i) and S(e) obtained in the same experimental conditions for soil kaolinites (Muller, 1988) were in the range 20–150 and 350–1500 a.u., respectively, i.e., one order of magnitude higher than for the hydrothermal samples studied here. The plot of the variation of S(d) values as a function of S(i) (Figure 7b) shows that S(d) values varied considerably for a given value of S(i). Similar trends were obtained by plotting S(d) vs. S(e). Thus, no direct relation exists between concentration of defect centers and substitutional Fe^{3+} content. The variation of the defect-center concentration through the studied alteration system appears to have been independent of the variation of the other two main crystal chemical characteristics of kaolinite—structural order and substitutional iron content. A similar observation was made for a weathering system previously studied (Muller and Calas, 1989).

https://doi.org/10.1346/CCMN.1990.0380605 Published online by Cambridge University Press

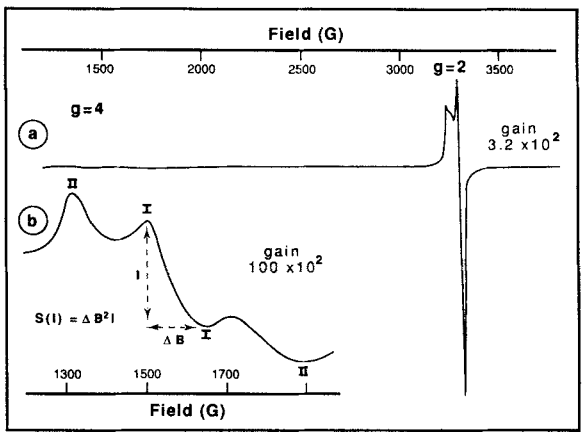

Figure 8. X-band electron paramagnetic resonance spectra at room temperature of fissural kaolinite inside breccia pipe. (a) Full-range spectra; note very weak signal in g = 4 region and very intense signal in g = 2 region, (b) expanded spectra of the signal in g = 4 region and calculation procedure for concentration of Fe^{3+} in "internal" substitutional site [S(i)].

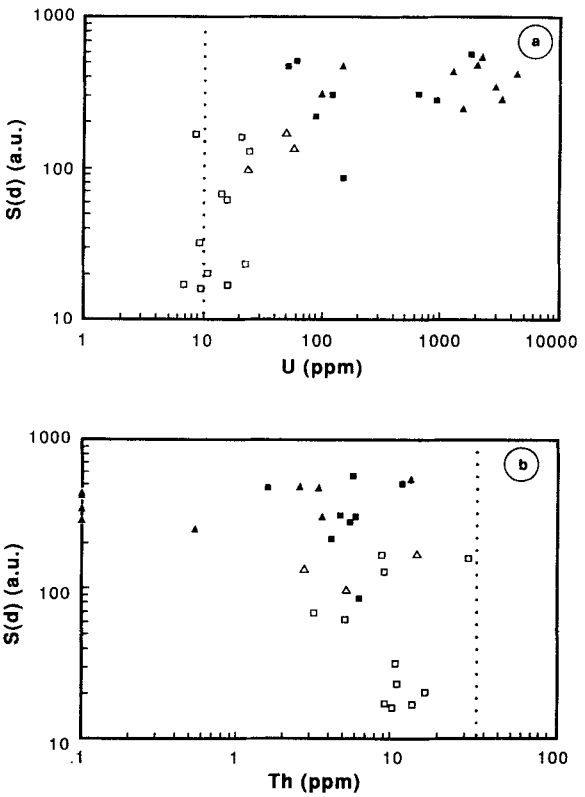

Figure 9. Plot of defect-center concentration [S(d)] vs. (a) total U content and (b) total Th content. For identification of symbols, see Figure 6. Dotted lines represent U and Th contents in unaltered Nopal rhyolitic tuff (Magonthier, 1987).

Correlations between defect-center concentration and U and Th content

Inasmuch as paramagnetic defect centers in kaolinite occur as a result of the natural irradiation generated by ^{238}U and ^{232}Th and their decay daughters (Muller and Calas, 1989), U and Th concentrations were systematically determined in all kaolinitic samples (Table 1). The variation of these concentrations as a function of the location of samples is presented in Table 1. Three major observations can be made: (1) all samples from the breccia pipe were significantly enriched in U relative to samples located outside of the breccia pipe, a clear-cut division for U concentrations corresponding to the faults which limit the breccia pipe; (2) the greatest U concentrations (>1000 ppm) correspond to samples in which kaolinite intimately coexisted with U-bearing minerals; (3) Th concentrations were very small in the samples collected within as well as outside of the breccia pipe.

A relation between defect-center concentration and U content is evidenced in Figure 9a: the greatest S(d) values correspond to samples characterized by the greatest U content. On the contrary, no correlation between S(d) and Th contents was observed (Figure 9b); however, detailed examination of Figure 9a, together with the data in Table 1, shows a relative dispersion of the data. Particularly, the defect concentration was as great [S(d) ≈ 500 a.u.] in samples containing 50–60 ppm of U (A2, A4a; Table 1) as in samples in which kaolinite intimately coexisted with U-bearing minerals and which contained 40–80 times more U (C3, C14). In the same way, S(d) values fluctuated by a factor of 5 between samples characterized by a same U-content (A4b and C1, [U] = 150 ppm, S(d) = respectively 86 and 475 a.u.; Table 1). This raises the question of the radiation source.

Radiation source for A- and A'-centers

The observations made on the kaolinites from the Sierra Peña Blanca range show that: (1) the greatest defect-center concentration [S(d) = 125–560 a.u.] was observed in samples from the breccia pipe having U contents of 60–4400 ppm; (2) A'-centers were clearly identified only in some of these samples containing >1000 ppm of U, i.e., samples containing XRD-detectable U^{6+}-bearing minerals (Table 1); (3) the crystallization of U^{6+}-bearing minerals was subsequent to the crystallization of kaolinite, according to the petrographic data. Thus, kaolinite from the breccia pipe appears to be an efficient fingerprint of two successive irradiations: (1) originally during the crystallization of kaolinite from radioactive hydrothermal solutions, and (2) permanently after the formation of, and in contact with, secondary U-silicates, which lead to the formation of A'-centers.

Furthermore, because of the high U/Th ratios, uranium appears to be the major radionuclide source to be considered. Obviously, the radioactive life of this

https://doi.org/10.1346/CCMN.1990.0380605 Published online by Cambridge University Press

element is by far too large to account for the observed radiation-induced centers: A- and A′-centers indicate the presence of short-lived daughter elements able to yield a significant irradiation of secondary minerals. If the system was closed for a time which was long relative to the half-life of the parent nuclide (10^7 years), the activities of all daughter nuclides should be equal to the activity of their respective parent; in this state of radioactive equilibrium, the defect-center concentration should be directly correlated to the measured U content. The absence of such a correlation (Figure 9a) may be interpreted as resulting from radioactive disequilibrium. Among the causes of such a disequilibrium, a loss of intermediate nuclides (for example, Ra) due to their greater solubility in water circulating in the fracture system must be considered. Whereas U-content measurements give only the present day U distribution, defect centers could be used to approach variations in radioactive disequilibrium during the history of alteration systems. This approach assumes that radiation efficiency as well as accurate dose-rate estimation are known (Clozel *et al.*, 1989).

CONCLUSION AND PERSPECTIVE

EPR is the method of choice to investigate defect centers, which generally occur in the ppm range and cannot be investigated with other methods. On the other hand, kaolinite appears to be highly sensitive to external irradiation, as indicated by the presence of defect centers even in samples devoid of significant radionuclide concentration. For example, EPR can detect the presence of minute quantities of kaolinite undetected by XRD.

In the model studied, point defect centers were strictly related to uranium decay series. Two types of centers were clearly identified: (1) A-centers were present in all the samples studied, as in all natural kaolinites, and were stable (to 400°C); (2) A′-centers were present in appreciable amounts only in kaolinite intimately coexisting with U-bearing minerals (or at U content >1000 ppm), and were destroyed at 350°C. Because of their different thermal stability, these different centers may be considered as formed at different periods: A′-centers, which annealed at moderate temperatures, are the most recent ones. This is in agreement with petrographic data, which showed that the crystallization of U^{6+}-bearing minerals was subsequent to the crystallization of kaolinite. Therefore, coupling between EPR and petrographic data allows successive irradiations of kaolinite to be linked to major changes in the geochemical environment of kaolinite during its history.

These results provide a unique tool for tracing the dynamics of the transfer of radionuclides in kaolinite-containing clayey formations: because of its great sensitivity to external irradiation, kaolinite could be used as a very sensitive *in situ* dosimeter. Particularly, it could provide unique means of estimating the content of short-lived radionuclides in alteration solutions. At the same time, as both concentration and type of defects created by natural irradiation are related to geochemical changes during kaolinite history, the intensity together with the shape of the point-defect-center signals allow an efficient fingerprint determination of successive generations of kaolinites during the weathering processes. From this point of view, the data obtained in this study validate the hypothesis proposed by Muller and Calas (1989) for the origin and concentration of A-centers in kaolinites from a laterite: the relatively great concentration of A-centers found in kaolinite intimately associated with iron oxides can be thought of as the memory of past accumulation of radionuclides adsorbed on the precursors (ferric gels) of these oxides. Finally, because many geological settings chosen for nuclear waste repositories are located in kaolinite-containing environments, point-defect-center dosimetry could be directly useful in safety assessments of these repositories (Ildefonse *et al.*, 1990).

ACKNOWLEDGMENTS

We are indebted to the Consejo de Recursos Minerales, Mexico (CRM), the Institut Français de Recherche Scientifique pour le Développement en Coopération (ORSTOM), and the Commissariat à l'Energie Atomique—Direction de l'Approvisionnement en Matières Nucléaires (CEA-DAMN) for the financial and logistic support of this work. C. R. Villasana and F. J. Altamirano (CRM), M. Portais (ORSTOM), and J. Dardel (CEA) are acknowledged for their personal support. B. Morin, A. El Ali, M. C. Sichère, A. Decarreau, M. Gautheyrou, and J. Dyon are thanked for technical assistance. We thank F. A. Mumpton and two anonymous reviewers for valuable comments on the manuscript.

REFERENCES

Alba, L. A. and Chavez, R. (1974) K-Ar ages from volcanic rocks from the Central Peña Blanca, Chihuahua, Mexico: *Isochron West* **10,** 21–23.

Angel, B. R., Jones, J. P. E., and Hall, P. L. (1974) Electron paramagnetic resonance studies of doped synthetic kaolinite. I: *Clay Miner.* **10,** 247–255.

Aniel, B. (1983) Les gisements uranifères associés au volcanisme acide Tertiaire de la Sierra Peña Blanca (Chihuahua, Mexique): *Geol. Geochim. Uranium Mem.* **2,** C.R.E.G.U., Nancy, France, 291 pp.

Calas, G. (1977) Les phénomènes d'altération hydrothermale et leur relation avec les minéralisations uranifères en milieu volcanique; le cas des ignimbrites tertiaires de la Sierra Peña Blanca, Chihuahua, Mexique: *Sci. Geol. Bull.* **30,** 3–18.

Calas, G. (1988) Electron paramagnetic resonance: in *Spectroscopic Methods in Mineralogy and Geology, Reviews in Mineralogy* **18,** F. C. Hawthorne, ed., Mineralogical Society of America, Washington, D.C., 513–571.

Cardenas-Flores, D. (1985) Volcanic stratigraphy and

U-Mo mineralization of the Sierra Peña Blanca district, Chihuahua, Mexico: in *Proc. Technical Committee Meeting on Uranium Deposits in Volcanic Rocks, El Paso, Texas, 1984,* I.A.E.A., Vienna, 125–136.

Cases, J. M., Lietard, O., Yvon, J., and Delon, J. F. (1982) Etude des propriétés cristallographiques, morphologiques, superficielles de kaolinites désordonnées: *Bull. Minéral.* **105,** 439–455.

Chaulot-Talmon, J. F. (1984) Etude géologique et structurale des ignimbrites du tertiaire de la Sierra Madre Occidentale, entre Hermosillo et Chihuahua, Mexique: Thesis, Univ. Orsay, Orsay, France, 260 pp.

Clozel, B., Muller, J. P., Dran, J. C., Hervé, J., and Calas, G. (1989) Study of alteration systems in the light of nuclear waste repository, 3. Radiation efficiency and dose rate estimation: in *Proc. E.U.G. V Congress, Strasbourg, 1989, Terra Abstr.* **1,** p. 112.

Cortes, M. R., Cruz, R. B., and Guerrero, S. P. (1980) Description petrografica de las mustras obtenidas de los nivelos cero y cuaranta del yacimineto Nopal I, Sierra Peña Blanca, municipio de Aldama, Chihuahua: in *Uramex Intern. Report, Informe* **10/80,** URAMEX, Mexico, 67 pp.

De Endredy, A. S. (1963) Estimation of free iron oxides in soils and clays by a photolytic method: *Clay Miner.* **5,** 209–217.

George-Aniel, B., Leroy, J., and Poty, B. (1985) Uranium deposits of the Sierra Peña Blanca, three examples of mechanisms of ore deposit formation in a volcanic environment: in *Proc. Technical Committee Meeting on Uranium Deposits in Volcanic Rocks, El Paso, Texas, 1984,* I.A.E.A., Vienna, 175–186.

Giese, R. F. (1988) Kaolin minerals. Structures and stabilities: in *Hydrous Phyllosilicates, Reviews in Mineralogy* **19,** S. W Bailey, ed., Mineralogical Society of America, Washington, D.C. 29–66.

Goodell, P. C. (1981) Geology of the Peña Blanca uranium deposit, Chihuahua, Mexico: in *Uranium in Volcanic and Volcaniclastic Rocks,* P. C. Goodell and A. C. Walters, eds., *A.A.P.G., Studies in Geology* **13,** 275–291.

Govindaraju, K. (1973) New scheme of silicate analysis (16 major, minor and trace elements) based mainly on ion exchange dissolution and emission spectrometry method: *Analysis* **2,** 367–376.

Hall, P. L. (1980) The application of electron spin resonance to studies of clay minerals. Isomorphous substitution and external surface properties: *Clay Miner.* **15,** 321–335.

Ildefonse, Ph., Muller, J. P., Cesbron, F., and Sichère, M. C. (1988) Mineralogy of uranium concentrations and associated hydrothermal alteration minerals in ignimbritic tuffs, Sierra Peña Blanca, Chihuahua, Mexico: *Geol. Soc. Amer. Abs. Progrs.* **20,** 7.

Ildefonse, Ph., Cesbron, F., Muller, J. P., and Calas, G. (1989) Study of alteration systems in the light of nuclear waste repository safety. 1. Element remobilization in hydrothermally altered tuffs: in *Proc. E.U.G. V Congress, Strasbourg, 1989, Terra Abstr.* **1,** 111–112.

Ildefonse, Ph., Muller, J. P., Clozel, B., and Calas, G. (1990) Study of two alteration systems as natural analogues for radionuclide release and migration: *Eng. Geol.* (in press).

Keller, W. D. (1976) Scan electron micrographs of kaolins collected from diverse environments or origin, I and II: *Clays & Clay Minerals* **24,** 107–117.

Leroy, J. L., Aniel, B., and Poty, B. (1987) The Sierra Peña Blanca (Mexico) and the Meseta Los Frailes (Bolivia): The uranium concentration mechanisms in volcanic environment during hydrothermal processes: *Uranium* **3,** 211–234.

Magonthier, M. C. (1984) Les ignimbrites de la Sierra Madre Occidentale et de la province uranifère de la Sierra Peña Blanca, Mexique: *Mem. Sci. Terre* **84-17,** Univ. Paris VI, Paris, 351 pp.

Magonthier, M. C. (1987) Relations entre les minéralisations d'uranium de la Sierra Peña Blanca (Mexique) et les ignimbrites porteuses: *Bull. Minéral.* **110,** 305–317.

Marfunin, A. S. (1979) *Spectroscopy, Luminescence and Radiation Centers in Minerals:* Springer-Verlag, Berlin, 352 pp.

Meads, R. E. and Malden, P. J. (1975) Electron spin resonance in natural kaolinites containing Fe^{3+} and other transition metal ions: *Clay Miner.* **10,** 313–345.

Mestdagh, M. M., Vielvoye, L., and Herbillon, A. J. (1980) Iron in kaolinite, II. The relationships between kaolinite crystallinity and iron content: *Clay Miner.* **15,** 1–14.

Muller, J. P. (1988) Analyse pétrologique d'une formation latéritique meuble du Cameroun. Essai de traçage d'une différenciation supergène par les paragénèses minérales secondaires: *Travaux et Documents Microfichés* **50,** ORSTOM, Paris, 664 pp.

Muller, J. P. and Bocquier, G. (1987) Textural and mineralogical relationships between ferruginous nodules and surrounding clayey matrices in a laterite from Cameroon: in *Proc. Int. Clay Conf., Denver, 1985,* L. G. Schultz, H. van Olphen, and F. A. Mumpton, eds., The Clay Minerals Society, Bloomington, Indiana, 186–196.

Muller, J. P. and Calas, G. (1989) Tracing kaolinites through their defect centers; kaolinite paragenesis in a laterite (Cameroon): *Econ. Geol.* **84,** 694–707.

(Received 19 July 1989; accepted 29 June 1990; Ms. 1928)